J Toxicol Pathol 2021; 34: 251–259

Case Report

A case report of RccHan™: WIST rat with multiple neoplastic and non-neoplastic proliferative lesions

Chisato Hayakawa[1*], Masayuki Kimura[1], Yusuke Kuroda[1], Seigo Hayashi[1], Kazuya Takeuchi[1], and Satoshi Furukawa[1]

[1] Toxicology and Environmental Science Department, Biological Research Laboratories, Nissan Chemical Corporation, 1470 Shiraoka, Shiraoka-shi, Saitama 349-0294, Japan

Abstract: It is extremely rare to have multiple spontaneous proliferative lesions in young adult rats. Here, we report the occurrence of different proliferative lesions in multiple tissues of a 7-week-old female rat in a 1-week repeated toxicity study. Grossly, multiple white patches and nodules in the bilateral kidneys, femoral and subcutaneous masses, and a nodule in the liver were observed. Renal lesions were diagnosed as renal mesenchymal tumors. One of the femoral subcutaneous masses was diagnosed as an adenolipoma consisting of mammary epithelial cells and mature adipocytes. The other femoral and abdominal subcutaneous masses were diagnosed as lipomas consisting of mature adipocytes. The liver nodule was diagnosed as non-regenerative hepatocellular hyperplasia, which was characterized by the proliferation of slightly hypertrophic hepatocytes. In the cauda equina, the growth of enlarged Schwann cells around the axon was observed, and this lesion was diagnosed as a neuroma. (DOI: 10.1293/tox.2021-0004; J Toxicol Pathol 2021; 34: 251–259)

Key words: renal mesenchymal tumor, adenolipoma, lipoma, neuroma, non-regenerative hepatocellular hyperplasia, rat

There are only few reports of multiple primary tumors in young rat[1, 2]. However, there are several reports of multiple primary tumors in humans[3, 4], but these cases were reported in the elderly, with few in young individuals. Here, we report a case wherein multiple primary neoplastic or non-neoplastic proliferative lesions were observed in the kidneys, mammary glands, soft tissues, cauda equina, and liver of a young rat.

This case was a female RccHan™: WIST rat at 7 weeks of age from a low-dose group in a 1-week repeated toxicity study. This female rat was obtained from Japan Laboratory Animals, Inc. at 5 weeks of age, and the study was conducted after 1-week of acclimation period. The rat was housed alone in a stainless steel cage at a temperature of 22 ± 3°C with 55% humidity (minimum 45%, maximum 70%) and 12 hour light/dark cycle, and was fed a solid diet (CRF-1; Oriental Yeast Co. Ltd., Japan) with drinking water *ad libitum*. After the end of dosing, the rat was euthanized through bleeding from the abdominal aorta under isoflurane anesthesia and necropsied. The kidneys, liver, brain, pituitary, spinal cord, femoral subcutaneous and abdominal subcutaneous masses were fixed with 10% neutral buffered formalin solution, embedded in paraffin, and sectioned. The sections were stained with hematoxylin and eosin (H&E), Masson's trichrome, Klüver-Barrera, and Alcian blue stains. Immunohistochemically, the specimens of the kidney were stained for vimentin, cytokeratin AE1/AE3 (CK AE1/AE3), desmin, alpha smooth muscle actin (α-SMA), S-100, Wilms' Tumor1 (WT1), CD117/c-kit, p63, and proliferating cell nuclear antigen (PCNA); the specimens of the femoral subcutaneous mass were stained for vimentin, CK AE1/AE3, α-SMA, and PCNA; the specimens of the cauda equina were stained for S-100, myelin protein zero (P0), p75 NGF receptor (p75NGFR), neurofilament protein, PCNA, and CD68; and the specimens of the liver nodule were stained for desmin, α-SMA, and PCNA, and further, the sections were subjected to a subsequent chromogenic reaction using the avidin-biotin complex method (Vectastain ABC Kit; Vector Laboratories, Burlingame, CA, USA)[5]. The primary antibodies used in this study are listed in Table 1. The toxicity study was conducted according to the Guidelines for Animal Experimentation, Biological Research Laboratory, Nissan Chemical Corporation.

Abnormal clinical signs were not observed. Macroscopically, multiple creamy-white patches (0.2–0.3 cm in diameter) and nodules (0.5 cm in diameter) were observed in the bilateral kidneys, and the cut surface of the nodule was bulging. Two femoral subcutaneous masses (1.7 cm and 2 cm in diameter, hereafter referred to as femoral subcutaneous masses I and II) were located in the left inguinal region. The femoral subcutaneous mass I appeared white-pink in color and solid, and the femoral subcutaneous mass II ap-

Received: 20 January 2021, Accepted: 5 April 2021
Published online in J-STAGE: 30 April 2021
*Corresponding author: C Hayakawa
(e-mail: hayakawac@nissanchem.co.jp)

peared creamy-white in color and soft. The abdominal subcutaneous mass (3.5 cm in diameter) was located in the center of the right side and appeared creamy-white in color and soft. A hepatic nodule (0.6 cm in diameter) was observed in the left lateral lobe and appeared reddish-brown in color and bulging (Fig. 1A–D).

Microscopically, multiple foci were observed in the outer medulla and cortex of the kidneys. In the foci, proliferating spindle and star-shaped cells with irregular-sized oval or round nuclei infiltrated between the pre-existing renal tubules (Fig. 2A and B) were observed, and the boundary between the foci and renal parenchyma was unclear. These cells exhibited fibroblast-like or myxoma-like cellular morphology. In some areas, vascular endothelium-like cells, characterized by flat cells with scanty cytoplasm, were observed (Fig. 2C). Additionally, regenerated renal tubules,

Table 1. Primary Antibodies Used in This Study

Antibody	Clone	Specificity	Supplier
Vimentin	V9	Monoclonal (mouse)	Dako (Tokyo, Japan)
Cytokeratin	AE1/AE3	Monoclonal (mouse)	Dako (Tokyo, Japan)
Desmin	D33	Monoclonal (mouse)	Dako (Kyoto, Japan)
α-smooth muscle actin	1A4	Monoclonal (mouse)	Dako (CA, USA)
S-100	-	Polyclonal (rabbit)	Dako (Tokyo, Japan)
Wilms tumor 1	6F-H2	Monoclonal (mouse)	Dako (CA, USA)
CD117/c-kit	-	Polyclonal (rabbit)	Dako (CA, USA)
p63	4A4	Monoclonal (mouse)	Abcam (Cambridge, UK)
PCNA	PC10	Monoclonal (mouse)	Dako (Glostrup, Denmark)
Myelin protein zero	-	Polyclonal (rabbit)	Abcam (Cambridge, UK)
p75 NGF Receptor	EP1039Y	Monoclonal (rabbit)	Abcam (Cambridge, UK)
Neurofilament	2F11	Monoclonal (mouse)	Dako (Glostrup, Denmark)
CD68	ED1	Monoclonal (mouse)	Millipore (USA)

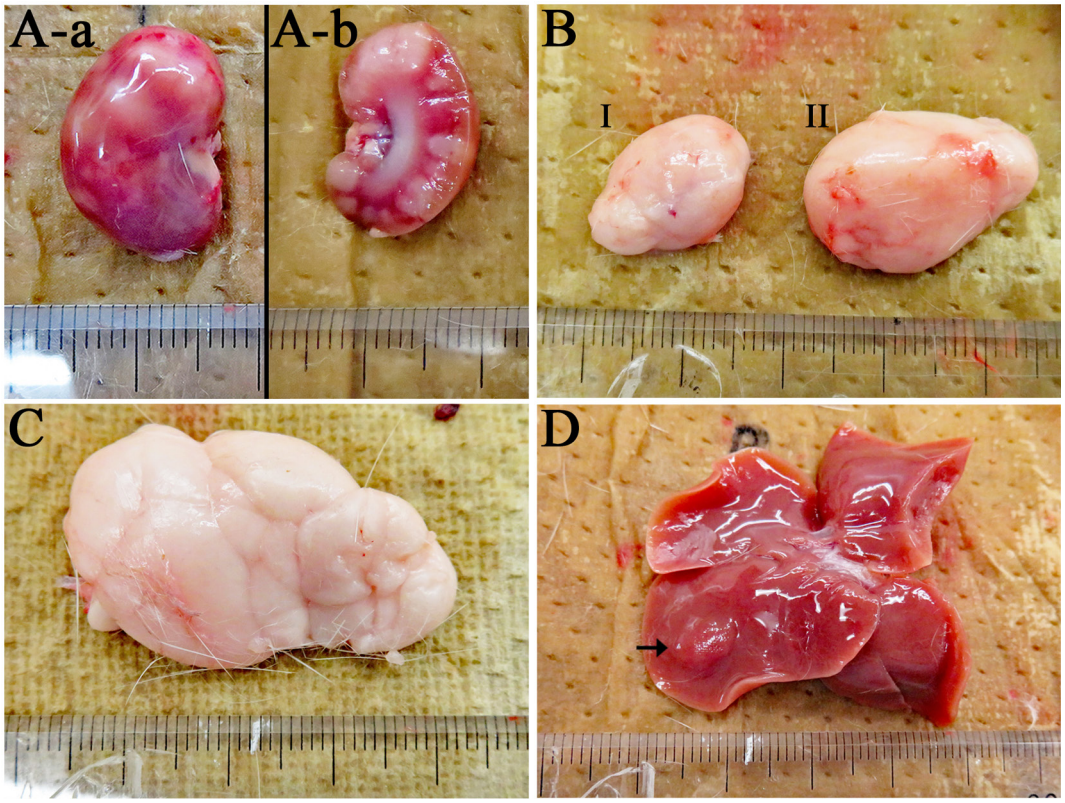

Fig. 1. Gross appearance of the kidney (A-a, A-b: cut surface), femoral subcutaneous masses I and II (B), abdominal subcutaneous mass (C), and liver (arrow: nodule) (D). Multiple creamy-white patches and nodules were observed in the bilateral kidneys, and the cut surface of the nodule was bulging. The femoral subcutaneous mass I appeared white-pink in color and solid, and the femoral subcutaneous mass II appeared creamy-white in color and soft. The abdominal subcutaneous mass appeared creamy-white in color and soft. A hepatic nodule was observed in the left lateral lobe and appeared reddish-brown in color and bulging.

large cystic tubules (Fig. 2D), and epithelial-like structures that differed from the existing tubules (Fig. 2E) were observed. Epithelial-like cells were characterized by cubic or columnar cells with poorly basophilic cytoplasm, partially exhibiting urothelium-like morphology, and few atypia and mitotic structures, and therefore, it appears like a primitive tubule. Mitotic structures of proliferating cells were highly observed in the infiltrating area (Fig. 2F). No histological transition from these epithelial-like cells to fibroblast-like, myxoma-like, or vascular epithelial-like cells was observed. Immunohistochemical analysis of rat renal tumors is summarized in Table 2. The fibroblast-like, myxoma-like, and vascular endothelial-like cells were positive for vimentin (Fig. 3A) and negative for CK AE1/AE3 (Fig. 3B), which were considered to be derived from the mesenchyme. These mesenchymal cells were remarkably positive for PCNA and exhibited high proliferative activity. The fibroblast-like and myxoma-like cells were desmin-positive (Fig. 3C) and partially α-SMA-positive (Fig. 3D), indicating myocyte differentiation. Additionally, some cells were S-100-positive (Fig. 3E), and the surrounding stroma of fibroblast-like cells appeared blue upon Masson's trichrome staining. Moreover, the surrounding stroma of myxoma-like cells appeared blue upon Alcian blue staining. The fibroblast-like and myxoma-

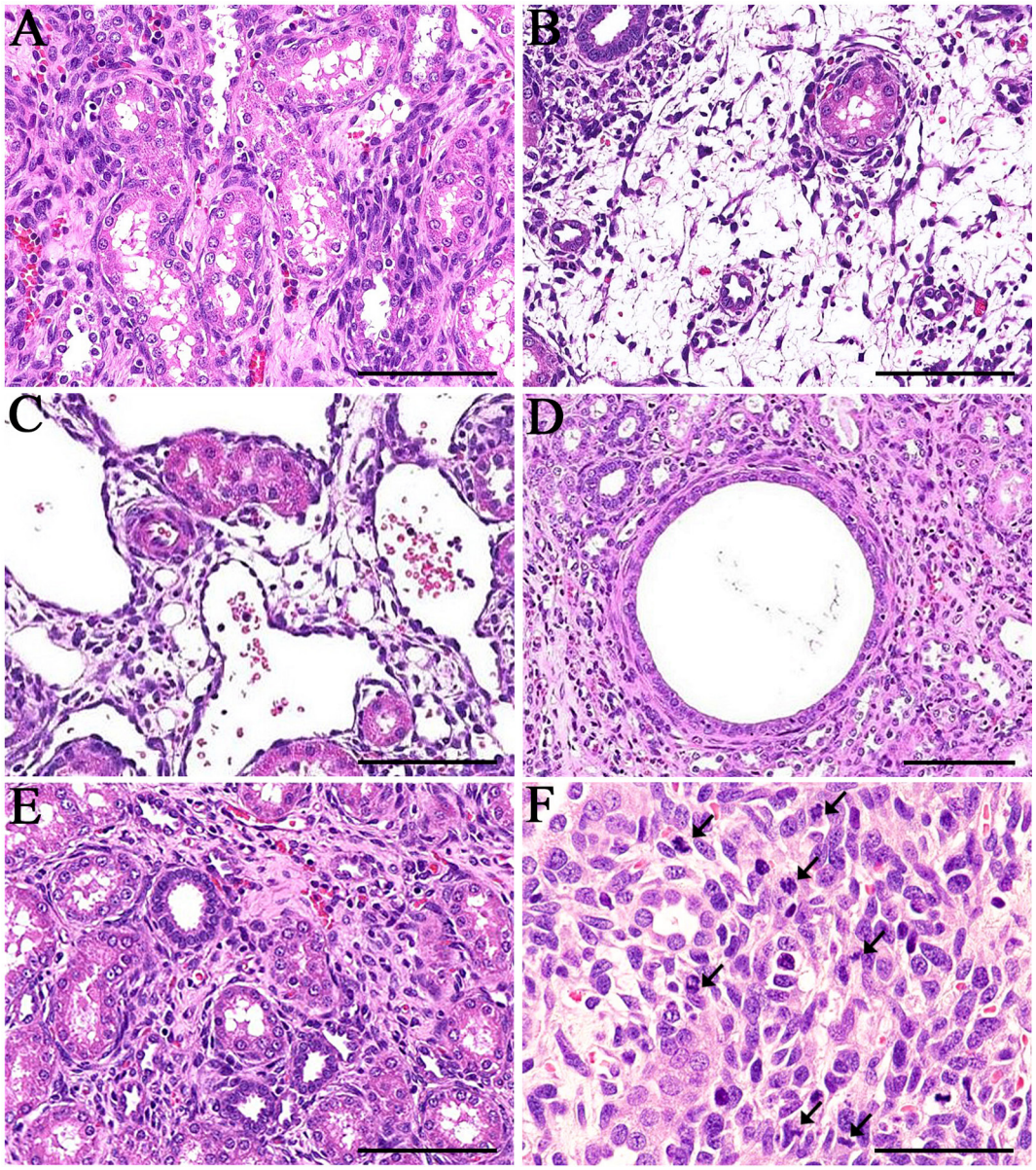

Fig. 2. Histology of the renal tumor. In the lesions, the proliferating spindle cells infiltrated between the pre-existing renal tubules (A). In some areas, star-shaped cells (B) and vascular endothelium-like cells (C), large cystic tubules (D), and epithelial-like structure of different morphology compared to the existing tubules (E) were observed. Mitotic structures of proliferating cells were highly observed in the infiltrating area (F, arrow). Hematoxylin and eosin (H&E) staining. Bar=100 µm.

Table 2. Immunohistochemical Analysis of Rat Renal Tumors

Antibody	This case	Renal mesenchymal tumor	Nephroblastoma
Vimentin	+	+	+
CK AE1/AE3	−	−	−/+
Desmin	+	−/+	−/+
α-SMA	+	+	−/+
S-100	+	−	−
WT1	+	+	+
CD117/c-kit	−	−	+

Grade signs − and + represent negative and positive, respectively.

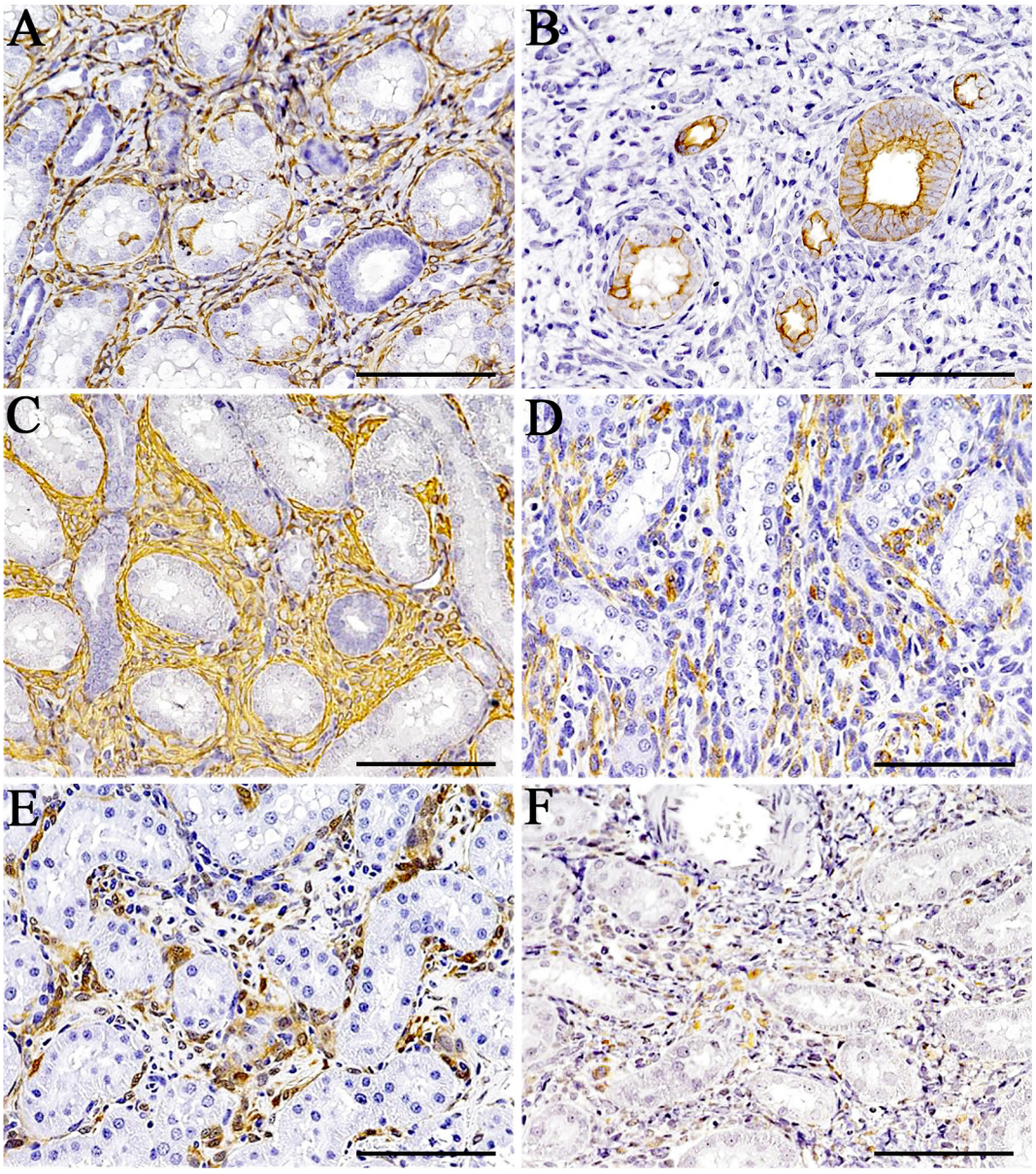

Fig. 3. Immunohistochemical findings of the renal tumor. The fibroblast-like cells were positive for vimentin (A) and desmin (C) and partially positive for α-SMA (D), S-100 (E), and WT1 (F), but negative for CK AE1/AE3 (B). Basophilic epithelial-like cells were positive for CK AE1/AE3 (B). Bar=100 µm.

like cells were partially WT1 positive (Fig. 3F), which is an indicator of renal mesenchymal tumors (RMT) and nephroblastomas in rats[6, 7]. All tumor cells were CD117/c-kit-negative, indicating positivity for blastemal components in rats[6]. Conversely, the basophilic epithelial-like cells and urothelium-like cells with glandular duct formation were CK AE1/AE3-positive (Fig. 3B) and vimentin-negative (Fig. 3A), indicating that they were epithelium-derived cells. Urothelium-like cells were p63-positive, suggesting differentiation into the urothelium because of their positivity as basal cells of the urothelium[8]. The proliferative activity of epithelial cells was not too high and was similar to that of the remaining normal renal tubules in the neoplastic lesions, and there was no clear transition between the mesenchymal and epithelial components, suggesting that these epithelial cells were a part of non-neoplastic component; they were considered as reactive hyperplasia or metaplasia of the remaining normal tubules. The renal lesions were diagnosed as RMT based on the following proliferating characteristics: mainly spindle cell proliferation around renal tubules and the presence of mesenchymal components consisting of a mixture of various cells. Spontaneously occurring RMTs are rare in rats of all ages[9–11]. It is the most characteristic feature is the absence of a neoplastic epithelial component. RMT is frequently misdiagnosed as nephroblastoma because the preexisting tubules often become hyperplastic and/or metaplastic, which is a morphology similar to that of nephroblastoma[9, 10]. Differential diagnoses include nephroblastoma, nephroblastematosis, and renal dysplasia. Nephroblastoma in rats is generally characterized by three proliferative elements: blastemic, epithelial, and stromal cells[12, 13]. The epithelial component often exhibits organoid differentiation into primitive glomeruli and/or tubules[9]. Differentiation into muscular, cartilaginous, osseous, or vascular tissues is not generally identified in rat nephroblastoma[9, 12]. Nephroblastematosis is considered as a precursor of nephroblastoma and is characterized by a small, solitary, and basophilic cell mass consisting of blast cells in the outer medulla, and is sometimes associated with primitive tubular and glomerular structures[10, 14]. The blastemal cells displace the existing renal tubules and form rosettes and alveolar structures. Nephroblastematosis is usually grossly invisible in rats; however, when grossly visible, it fully develops into neoplastic tissue, that is, nephroblastoma[14, 15]. Renal dysplasia is a developmental anomaly in the kidneys, and renal components are often present with hypoplasia. Histologically, embryonic glomerular and tubular structures are present, and sometimes, they include mesenchymal components, such as cartilage in the stroma[16]. In the present case, the masses differentiated from nephroblastoma, nephroblastematosis, and renal dysplasia because of its different growth patterns and histological features.

The femoral subcutaneous mass I comprised mature adipose tissues and islands of mammary glands and was surrounded by fibrous capsules (Fig. 4A). The constituent epithelium of the mammary glands was stratified and basophilic, with irregularly sized nuclei (Fig. 4B). Mitotic figures of epithelial cells were frequently observed. Mast cells and fibroblasts were observed in the interlobular connective tissues. The mammary epithelial cells were CK AE1/AE3-positive (Fig. 4C) and vimentin-negative (Fig. 4D), and the myoepithelial cells were α-SMA-positive (Fig. 4E), while the adipose cells were vimentin-positive (Fig. 4D). In general, mammary glands of young rats are under developed, and the terminal bud of mammary glands (called the terminal end bud: TEB) are present with stratifying epithelial cells exhibiting high proliferative activity, particularly at around 7 weeks of age, and these are considered as normal structures during development[17, 18]. Given the characteristic mature adipocytes and mammary epithelial cells here, we diagnosed it as mammary adenolipoma. Mammary adenolipomas are rare tumors identified in rats[19, 20]. Histologically, such neoplasms consist of epithelial cells, mature adipocytes, and fibrous tissues[19, 21]. A synonym is a benign mixed tumor (adenolipoma type). The present case exhibited similar histological characteristics.

The grossly observed femoral subcutaneous mass II and abdominal subcutaneous mass were characterized by diffused proliferation of mature adipocytes, which were surrounded by a fibrous capsule and diagnosed as lipoma.

Lesions in the cauda equina were found incidentally through histopathological examination, which were characterized by the presence of a large nerve bundle-like structure in the spinal cavity (Fig. 5A, arrow), and consisted mainly of Schwann cells, fibroblasts, and perineurium cells (Fig. 5B). Schwann cells proliferated around the normal axons and were characterized by moderately large round nuclei with no mitotic structures and were not associated with onion-bulb-like structures (Fig. 5C). Spindle-shaped cells, which seemed to be fibroblasts, proliferated in the endoneurium. Schwann cells were S-100-positive (Fig. 5D). Schwann cells and perineurium cells were positive for p75NGFR (Fig. 5E). Axons were neurofilament-positive (Fig. 5F), myelin sheaths were P0-positive (Fig. 5G) and appeared blue upon Klüver-Barrera staining (Fig. 5H). Most cells were negative for PCNA, and a few macrophages were positive for CD68. These lesions were present in the spinal cavity and exhibited low proliferative activity, while proliferating Schwann cells formed around myelinated nerve fibers in a bundle. Therefore, we diagnosed the proliferating lesions as a neuroma. Neuroma is a reactive, non-neoplastic proliferative lesion of peripheral nerves. Histologically, it consists of proliferative Schwann cells surrounding the axons and connective tissue, including perineurium cells[22–24]. Differential diagnoses include Schwannoma, neurofibroma, and intraneuronal perineuroma, all of which are neoplastic lesions and characterized by monotonous tumor cell proliferation, which does not proliferate along with other cellular components, such as Schwann cells, myelinated nerves, perineurium cells, and fibrous connective tissue. Additionally, we diagnosed the present case as non-traumatic neuroma, since there were no findings suggestive of trauma, and thus, we suspected that it may be due to some congenital genetic abnormalities, since proliferative lesions were observed in various tissues of this

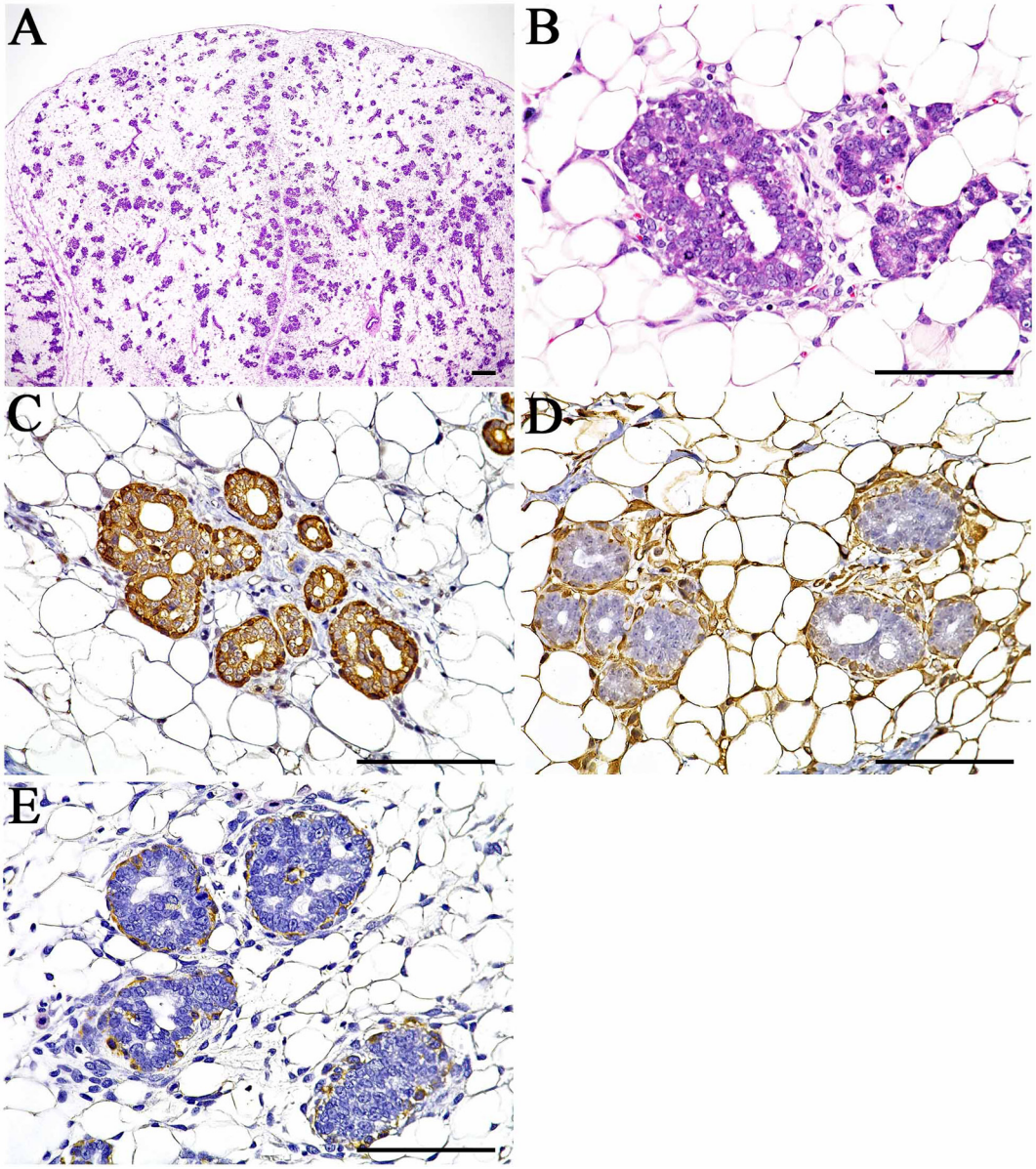

Fig. 4. H&E (A and B) and immunohistochemical (C–E) staining of femoral subcutaneous mass I. (A) The mass comprised mature adipose tissues and island of mammary glands and was surrounded by a fibrous capsule. Bar=400 µm. (B) Mammary epithelial cells were stratified and basophilic, with irregularly sized nuclei. Bar=100 µm. (C) The mammary epithelial cells were positive for CK AE1/AE3. Bar=100 µm. (D) Adipose cells were positive for vimentin. Bar=100 µm. (E) Myoepithelial cells were positive for α-SMA. Bar=100 µm.

young rat. There are no reports of non-traumatic neuromas in rats; however, there are some reports in humans[23, 25, 26]. Some authors report that non-traumatic neuromas in humans are congenital due to the lack of traumatic history[27].

A grossly observed hepatic nodule was characterized by the massive proliferation of slightly hypertrophic hepatocytes with mild compression towards the adjacent hepatocytes (Fig. 6A); and these hepatocytes were similar to the normal hepatocytes with no cellular atypia (Fig. 6B). Most of these cells were positive for PCNA, suggesting higher proliferative activity than the surrounding normal hepatocytes (Fig. 6C). Based on the above findings, we diagnosed it as non-regenerative hepatocellular hyperplasia. Additionally, many desmin- and α-SMA-positive cells, which were considered to be Ito cells transformed into myofibroblasts, were found to be present in the hyperplastic area. Non-regenerative hepatocellular hyperplasia has been reported as a spontaneous change observed in aged rats and is extremely rare in young rats.

In this study, we report a very rare case with five proliferative lesions consisting of a renal mesenchymal tumor, mammary adenolipoma, lipoma, neuroma, and non-regenerative hepatocellular hyperplasia, at 7 weeks of age. It has been reported that multiple cancers in humans are caused by congenital genetic abnormalities[28]. Although the cause of these lesions was unclear, we believe that their occurrence

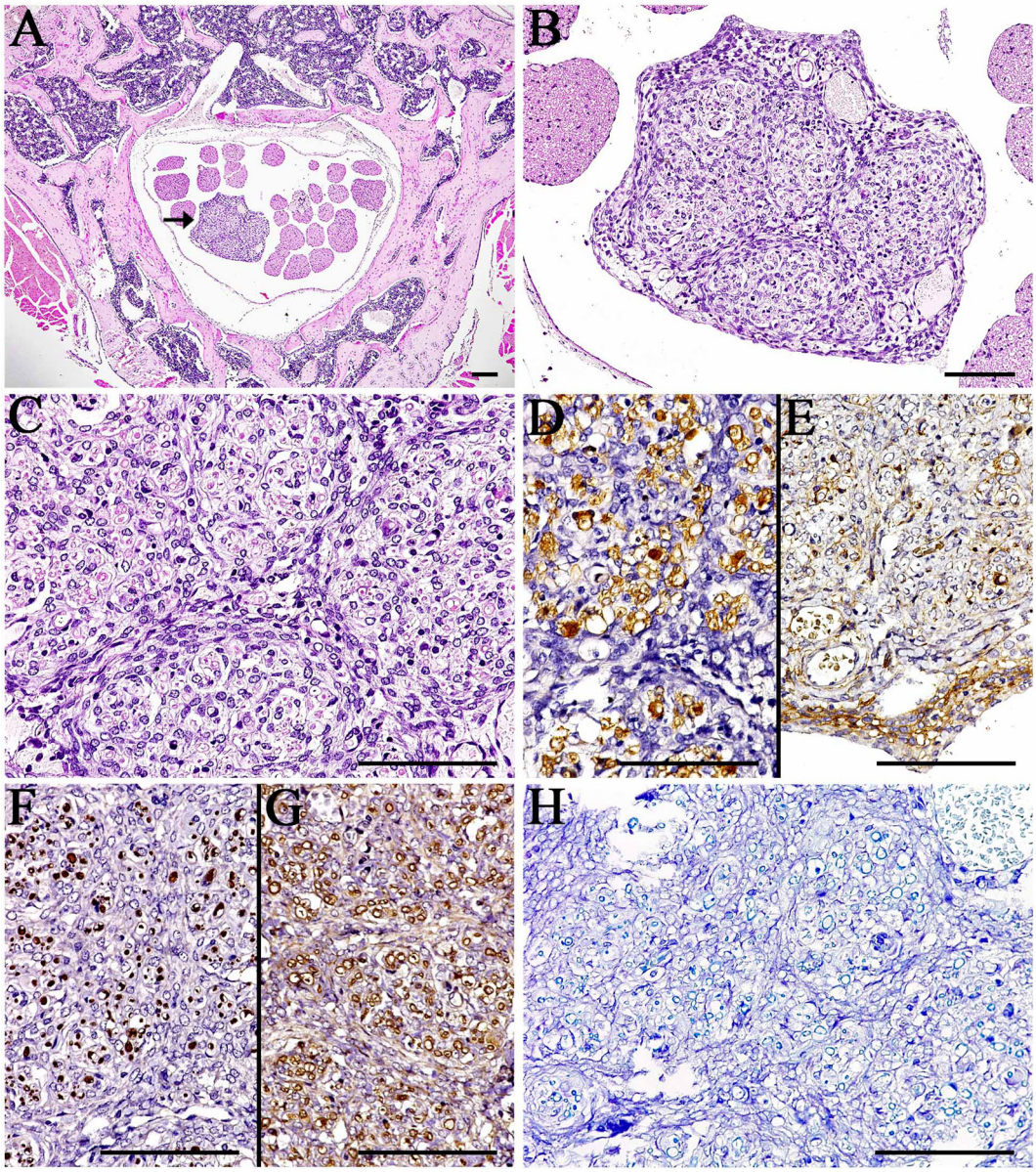

Fig. 5. H&E (A–C) and immunohistochemical (D–H) staining of lesions in the cauda equine. (A) The lesions were characterized by the presence of a large nerve bundle-like structure in the spinal cavity (arrow). Bar=200 µm. (B) The main components were Schwann cells, fibroblasts, and perineurium cells. Bar=100 µm. (C) Schwann cells proliferated around the normal axons and were characterized by moderately large rounded nuclei with no mitotic structures and were not associated with onion-bulb like structures. Bar=100 µm. (D) Schwann cells were positive for S-100 protein. Bar=100 µm. (E) Schwann and perineurium cells were positive for p75NGFR. Bar=100 µm. (F) Axons were positive for neurofilament. Bar=100 µm. (G and H) Myelin sheaths were P0 positive (G), and appeared blue upon Klüver-Barrera staining (H). Bar=100 µm.

is likely due to congenital genetic abnormalities, which is attributed to the presence of multiple proliferated lesions in this young rat.

Disclosure of Potential Conflicts of Interest: The authors declare that they have no conflicts of interest.

Acknowledgements: The authors thank Dr. Kiyokazu Ozaki (Department of Pathology, Faculty of Pharmaceutical Sciences, Setsunan University), Dr. Katsuhiko Yoshizawa (Department of Food Sciences and Nutrition, Mukogawa Women's University), and Dr. Hijiri Iwata (LunaPath LLC) for providing important suggestions, as well as Ms. Kaori Maejima and Mr. Makoto Tsuchiya for their excellent technical assistance.

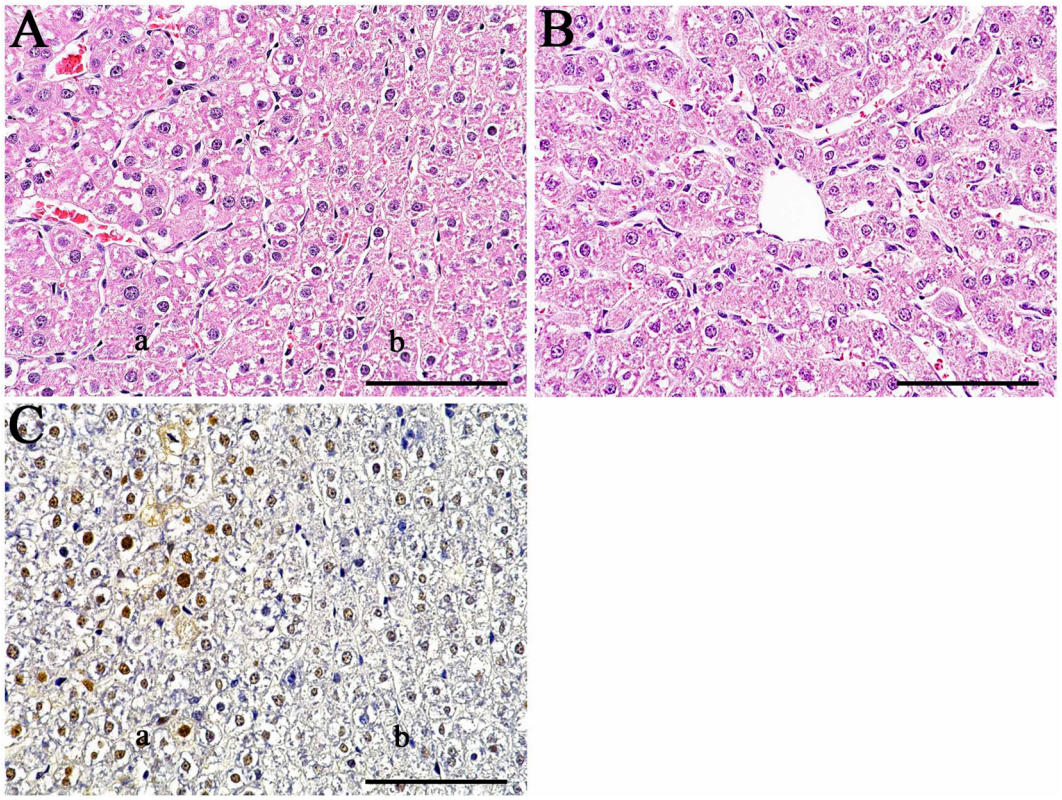

Fig. 6. H&E (A and B) and immunohistochemical (C) staining of the hepatic nodule. (A and B) The hepatic nodule was characterized by the massive proliferation of slightly hypertrophic hepatocytes with mild compression towards the adjacent hepatocytes (A-a: lesion, A-b: normal). Moreover, they were not associated with cell atypia and were similar to the normal hepatocytes (B). Bar=100 µm.
(C) Most of these cells were positive for PCNA, suggesting higher proliferative activity than the surrounding normal hepatocytes (a: lesion, b: normal). Bar=100 µm.

References

1. Ikezaki S, Takagi M, and Tamura K. Natural occurrence of neoplastic lesions in young sprague-dawley rats. J Toxicol Pathol. **24**: 37–40. 2011. [Medline] [CrossRef]
2. Son WC, Bell D, Taylor I, and Mowat V. Profile of early occurring spontaneous tumors in Han Wistar rats. Toxicol Pathol. **38**: 292–296. 2010. [Medline] [CrossRef]
3. Williamson CW, Paravati A, Ghassemi M, Lethert K, Hua P, Hartman P, and Sanghvi P. Five simultaneous primary tumors in a single patient: a case report and review of the literature. Case Rep Oncol. **8**: 432–438. 2015. [Medline] [CrossRef]
4. Testori A, Cioffi U, De Simone M, Bini F, Vaghi A, Lemos AA, Ciulla MM, and Alloisio M. Multiple primary synchronous malignant tumors. BMC Res Notes. **8**: 730. 2015. [Medline] [CrossRef]
5. Moroki T, Matsuo S, Hakeyama H, Hayashi S, Matsumoto I, Suzuki S, Kotera T, Kumagai K and Ozaki K. Databases for technical aspects of immunohistochemistry—2021 update. J Toxicol Pathol. **34**: 161–181. 2021.
6. Yoshizawa K, Kinoshita Y, Emoto Y, Kimura A, Uehara N, Yuri T, Shikata N, and Tsubura A. N-Methyl-N-nitrosourea-induced renal tumors in rats: Immunohistochemical comparison to human wilms tumors. J Toxicol Pathol. **26**: 141–148. 2013. [Medline] [CrossRef]
7. Ito Y, Matsushita K, Tsuchiya T, Kohara Y, Yoshikawa T, Sato M, Kitaura K, and Matsumoto S. Spontaneous nephroblastoma with lung metastasis in a rat. J Toxicol Pathol. **27**: 91–95. 2014. [Medline] [CrossRef]
8. Truong LD, and Shen SS. Immunohistochemical diagnosis of renal neoplasms. Arch Pathol Lab Med. **135**: 92–109. 2011. [Medline] [CrossRef]
9. Seely JC. Renal mesenchymal tumor vs nephroblastoma: revisited. J Toxicol Pathol. **17**: 131–136. 2004. [CrossRef]
10. Frazier KS, Seely JC, Hard GC, Betton G, Burnett R, Nakatsuji S, Nishikawa A, Durchfeld-Meyer B, and Bube A. Proliferative and nonproliferative lesions of the rat and mouse urinary system. Toxicol Pathol. **40**(Suppl): 14S–86S. 2012. [Medline] [CrossRef]
11. Hard GC. Mesenchymal tumor, kidney, rat. In: Urinary System, 2nd ed. TC Jones, GC Hard, and U Mohr (eds). Springer, Berlin, Heidelberg, New York. 118–129. 1998.
12. Cardesa A, and Ribalta T. Nephroblastoma, kidney, rat. In: Urinary System, 2nd ed. TC Jones, GC Hard, and U Mohr (eds). Springer, Berlin, Heidelberg, New York. 129–138. 1998.
13. Jackson CB, and Kirkpatrick JB. Nephrogenic rest in a Crl:CD (SD)IGS BR rat. Vet Pathol. **39**: 588–589. 2002. [Medline] [CrossRef]
14. Kalaiselvan P, Mathur KY, Pande VV, Madheswaran R, Bhelonde JJ, Shelar PD, Udupa V, and Shingatgeri VM. In-

tralobar nephroblastematosis in a nine-week-old Wistar rat. Toxicol Pathol. **37**: 819–825. 2009. [Medline] [CrossRef]
15. Mesfin GM. Intralobar nephroblastematosis: precursor lesions of nephroblastoma in the Sprague-Dawley rat. Vet Pathol. **36**: 379–390. 1999. [Medline] [CrossRef]
16. Ruehl-Fehlert CI, Deschl U, Kayser M, and Hartmann E. Bilateral noncystic renal dysplasia in a Wistar-rat. Exp Toxicol Pathol. **54**: 293–299. 2003. [Medline] [CrossRef]
17. Russo J, and Russo IH. Influence of differentiation and cell kinetics on the susceptibility of the rat mammary gland to carcinogenesis. Cancer Res. **40**: 2677–2687. 1980. [Medline]
18. Russo IH, and Russo J. Mammary gland neoplasia in long-term rodent studies. Environ Health Perspect. **104**: 938–967. 1996. [Medline] [CrossRef]
19. Germann PG, and Ernst H. Mammary adenolipoma in a female Sprague-Dawley rat. Exp Toxicol Pathol. **45**: 67–69. 1993. [Medline] [CrossRef]
20. Ide T, Cho YM, Oishi Y, and Ogawa K. Spontaneous adenolipoma of the mammary gland in a male F344 rat. J Toxicol Pathol. **34**: 231–234. 2021.
21. Rudmann D, Cardiff R, Chouinard L, Goodman D, Küttler K, Marxfeld H, Molinolo A, Treumann S, Yoshizawa K. INHAND Mammary, Zymbal's, Preputial, and Clitoral Gland Organ Working Group Proliferative and nonproliferative lesions of the rat and mouse mammary, Zymbal's, preputial, and clitoral glands. Toxicol Pathol. **40**(Suppl): 7S–39S. 2012. [Medline] [CrossRef]
22. Kaufmann W, Bolon B, Bradley A, Butt M, Czasch S, Garman RH, George C, Gröters S, Krinke G, Little P, McKay J, Narama I, Rao D, Shibutani M, and Sills R. Proliferative and nonproliferative lesions of the rat and mouse central and peripheral nervous systems. Toxicol Pathol. **40**(Suppl): 87S–157S. 2012. [Medline] [CrossRef]
23. Tsitouridis J, Kouklakis G, Xiarhos P, and Patakiuta F. Non traumatic neuroma of the bile duct: report of a case. Dig Endosc. **10**: 323–326. 1998. [Medline] [CrossRef]
24. Tanaka A, Gonzalez-Alva P, Oku Y, Yoshizawa D, Ito S, Ide F, Sakashita H, and Kusama K. Histopathological findings of peripheral nerve sheath lesions in the oral region. J Meikai Dent Med. **36**: 117–186. 2007.
25. McGuire LS, Behbahini M, Das S, Loeffler D, Burger P, Engelhard H, Valyi-Nagy T, and Mehta A. Intramedullary amputation neuroma: a case report and review of the literature. Clin Neuropathol. **36**: 73–77. 2017. [Medline] [CrossRef]
26. Parres C, Thomas C, Ooi W, Bryan D, Ho D, and Srinivasan J. Nontraumatic hypertrophic neuroma in treated Hansen disease. Neurology. **82**: 93–94. 2014. [Medline] [CrossRef]
27. Santagata S, Tuli S, Wiese DE 2nd, Day A, and De Girolami U. Intramedullary neuroma of the cervicomedullary junction. Case report. J Neurosurg Spine. **5**: 362–366. 2006. [Medline] [CrossRef]
28. Toyoizumi T, Myrai R, Shioya N, Ikeuchi K, Ishikawa M, Yamazaki Y, and Aoki T. A case of triple cancers (stomach, kidney and rectum) with many benign neoplasms. Progress of Digestive Endoscopy. **51**: 104–107. 1998. [CrossRef]